Hydrol. Earth Syst. Sci., 30, 7257–7264, 2026
https://doi.org/10.5194/hess-30-7257-2026
© Author(s) 2026. This work is distributed under
the Creative Commons Attribution 4.0 License.

Hydrology and Earth System Sciences
Open Access
EGU

LESSONS report: Fine-scale representation of consecutive dry days

Benjamin Poschlod[1,2], **Lukas Brunner**[2], **and Jana Sillmann**[2]

[1]Institute for Global Water Security, Hamburg University of Technology, Hamburg, 21079, Germany
[2]Research Unit Sustainability and Climate Risks, Earth and Society Research Hub (ESRAH), Universität Hamburg, Hamburg, 20144, Germany

Correspondence: Benjamin Poschlod (benjamin.poschlod@tuhh.de)

Received: 6 July 2026 – Discussion started: 21 August 2026
Revised: 19 October 2026 – Accepted: 13 November 2026 – Published: 24 November 2026

Abstract. The number of consecutive dry days (CDD) is a widely used metric for assessing meteorological drought. This study investigates spatial CDD patterns over Germany during the drought year of 2018, comparing a convection-permitting model (CPM) at 3 km resolution with ERA5 reanalysis at 31 km, gauge-based interpolated observations at 1 km, and radar measurements at 1 km. The analysis reveals a *surprise*: high-resolution CPM and radar data produce strikingly heterogeneous, "brushstroke-like" spatial structures that differ fundamentally from the smooth fields of reanalysis and gridded observations.

Our report confirms that these sharp spatial discontinuities are not computational artifacts but a physical consequence of the sensitivity to the fixed daily dryness threshold of the CDD metric. We find that the CPM can well reproduce these fine-scale patterns that are also detected by radar measurements, which is quantified by a spatial autocorrelogram and the radially averaged power spectral density.

While averaging CDD over multiple years smooths out the brushstroke patterns, such temporal averaging does not resolve the underlying *shortcoming*: multi-year CDD is built upon individual annual CDD values that are, as shown here, highly variable and strongly dataset-dependent. A statistic whose single-year realizations are dominated by threshold-crossing noise provides an unstable foundation for climatological analysis regardless of the aggregation period applied. As a *lesson* learnt, CDD depends on the spatial resolution of the data and, at the kilometre scale, on single precipitation events close to the threshold; CDD should therefore only be compared between data sets of similar resolution and interpreted with caution at individual grid cells or stations, including in drought monitoring, impact assessment, and climate model evaluation. This study reports on the surprising fine-scale spatial patterns and resulting shortcomings of the CDD metric and is therefore submitted as a LESSONS report, a paper category dedicated to documenting Limitations, Errors, Surprises, Shortcomings, and Opportunities for New Science.

1 Introduction

Droughts are one of the most expensive hazards, potentially triggering a wide range of ecological, economic, and societal risks (AghaKouchak et al., 2023). Meteorological droughts, i.e. periods with a deficit of precipitation relative to normal conditions (Van Loon and Van Lanen, 2012), can thereby induce a cascade towards agricultural, surface water and groundwater droughts (Liu et al., 2023). Various indices exist to assess meteorological droughts (Kchouk et al., 2022), where the number of consecutive dry days (CDD) is a simple and widely used metric defined by the Expert Team on Climate Change Detection and Indices (ETCCDI; Zhang et al., 2011). CDD is used to assess meteorological drought in the IPCC AR6 (Intergovernmental Panel On Climate Change (IPCC), 2023) and in global projections of dry spells (Petrova et al., 2024), which rely on grids of about 100 km; kilometre-scale models yield shorter dry spells when remapped to such grids (Wille et al., 2025).

While droughts are typically considered as a large-scale phenomenon, drought indices may show spatial fine-scale variability (Gebrechorkos et al., 2023). Recent global analyses of kilometre-scale models confirm that the spatial subgrid variability of ETCCDI extreme indices – including consecutive wet days, the wet-day counterpart of CDD – is largely lost at the coarse resolution of conventional global

climate models (Brunner et al., 2025). Here, we aim to explore the spatial patterns of CDD in high-resolution data sets including a convection-permitting model (CPM) simulation. CPMs at resolutions of less than 4 km explicitly resolve convective processes instead of using a parametrization (Lucas-Picher et al., 2021), which is considered a "step change" in understanding local climate and impacts compared to conventional regional climate models (Kendon et al., 2021). CPMs better capture complex topography and land surface heterogeneities (Gutowski et al., 2020) and are found to improve representation of temperature over complex terrain (Karki et al., 2017). CPMs resolve storms and improve the representation of clouds and solar radiation (Hentgen et al., 2019), the daily cycle of precipitation (Lind et al., 2020), the frequency and intensity of precipitation (Ban et al., 2021), topography effects on extreme precipitation (Dallan et al., 2023; Poschlod and Koh, 2024), wind systems (Molina et al., 2024), snow depth (Monteiro et al., 2024; Poschlod and Daloz, 2024), and droughts (Akinsanola et al., 2024). For the representation of spatial CDD patterns, we here compare a CPM simulation to ERA5 reanalysis, gridded observations, and bias-adjusted radar measurements over Germany. We find a surprising spatial pattern providing lessons for future model evaluation and the use of the CDD metric.

2 Data and Methods

We use four different precipitation data sets over Germany: (1) ERA5 reanalysis (Hersbach et al., 2020) at 0.25° equalling $\sim$31 km, (2) convection-permitting simulations of COSMO-CLM at 3 km, nested directly into ERA5, which provides the lateral boundary conditions every hour (Brienen et al., 2022; Rybka et al., 2023), (3) gridded observations of quality-checked rain gauge measurements (HYRAS) at 1 km, obtained by interpolating the ratio between daily gauge precipitation and a background field from multiple linear regression with inverse distance weights of the four nearest gauges (Rauthe et al., 2013), and (4) the radar-based precipitation reanalysis RADKLIM. RADKLIM consists of quality-checked and artifact-corrected radar measurements at 1 km, where the intensity is adjusted with the observed precipitation from rain gauges (Winterrath et al., 2017). In this short report, we mainly focus our analysis to the year 2018, reflecting severe drought conditions over Europe (Blauhut et al., 2022). We aggregate all data sets to daily resolution and calculate CDD following the ETCCDI, counting the largest number of consecutive days with precipitation below 1 mm within one year. CDD are calculated using the package *xclim* (Bourgault et al., 2023) in Python 3.8.

For a further analysis of spatial variability of CDD fields, we remap the finer-resolution observational daily precipitation data from 1 km to the coarser 3 km grid of COSMO-CLM using bilinear interpolation (*remapbil* in CDO; Schulzweida, 2026) and re-calculate the CDD. We compute global Moran's I across a range of spatial scales by defining neighbourhoods as all grid cells within a circle of radius r, for $r = 3$ to 99 km, yielding a spatial autocorrelogram for scale-dependent comparison of CDD patterns between the three high-resolution datasets; Moran's I correlates the value of each grid cell with those of its neighbours, from about -1 (dispersed) via 0 (random) to 1 (clustered). Further, we calculate the radially averaged power spectral density (RAPSD; Sinclair and Pegram, 2005) by applying a 2-D fast Fourier transform to the CDD fields, constraining the analysis to the largest square of valid CDD values (333 km $\times$ 333 km) to avoid artefacts from no-data gaps. The spatial mean is subtracted prior to the transform to suppress the zero-frequency component, and the resulting power spectrum is averaged radially in wavenumber space using the package *pysteps* (Pulkkinen et al., 2019). RAPSD is commonly used to evaluate the spatial structure of precipitation fields across scales (Ravuri et al., 2021) and complements Moran's I by decomposing total variance continuously across wavelengths, allowing dataset differences to be attributed to specific spatial scales.

3 Spatial patterns of consecutive dry days

The spatial distribution of CDD for 2018 is shown in Fig. 1 for all four datasets at their native resolution. Within the common domain of all data sets, CDD values range from 11 to 68 d (Table S1 in the Supplement). ERA5 exhibits a smooth, coarse-grained pattern reflecting its comparatively low spatial resolution (Fig. 1a), whereas the convection-permitting simulation COSMO-CLM at 3 km produces a strikingly heterogeneous field with elongated, anisotropic, brushstroke-like structures (Fig. 1b).

The gridded observational dataset HYRAS displays a slightly smoother pattern with quasi-circular, blob-like anomalies ("bull's-eyes") of alternating higher and lower CDD values superimposed (Fig. 1c). The radar-based RADKLIM product closely resembles the fine-scale spatial variability of COSMO-CLM (Fig. 1d). We note that a direct evaluation of CDD magnitudes at individual grid cells is not the focus of this study, as the reanalysis and convection-permitting simulation are freely evolving atmospheric models that – despite being constrained by observed boundary conditions – will not reproduce observed precipitation at the correct locations due to internal climate variability. Rather, our interest lies in the characteristics of the spatial fine-scale structure of the CDD patterns.

The spatial pattern visible in Fig. 1b was initially unexpected for a hydro-climatic variable, prompting us to verify the CDD calculation. The pattern was confirmed to be robust across multiple years and an independent convection-permitting simulation using the WRF model (Collier and Mölg, 2020; see Fig. S1), and independent CDD implemen-

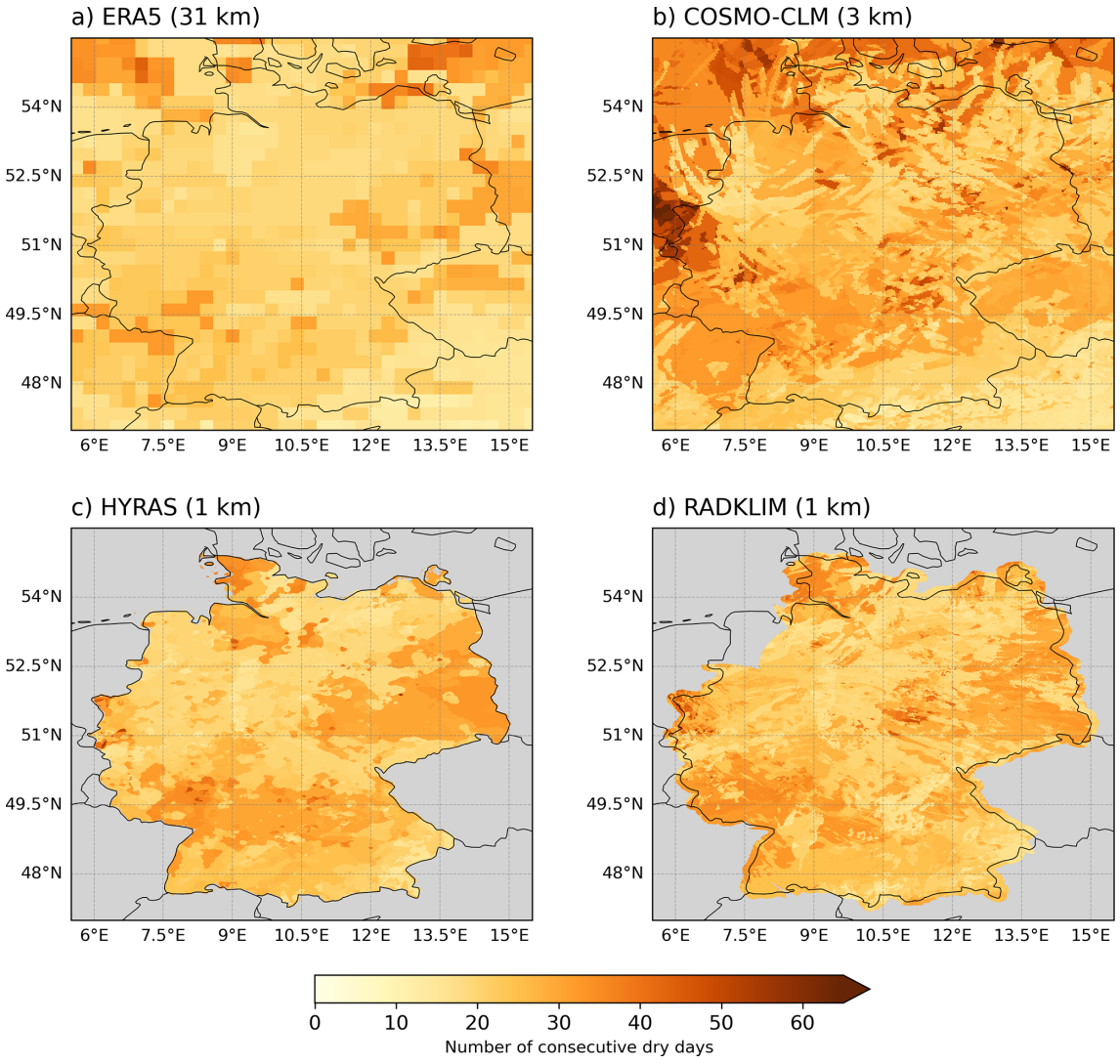


Figure 1. Number of consecutive dry days in 2018 for ERA5 reanalysis **(a)**, convection-permitting simulations of COSMO-CLM **(b)**, HYRAS gridded observations **(c)**, and intensity-adjusted radar measurements of RADKLIM **(d)**. Values above 65 d, which occur at fewer than 0.02 % of the grid cells over Germany, are shown in the darkest colour; grey areas indicate no data. COSMO-CLM simulates a dry anomaly over the Benelux countries and western Germany, which is absent from ERA5, HYRAS and RADKLIM. Mean CDD over the largest common domain of all four data sets: 21.0 (ERA5), 26.8 (COSMO-CLM), 24.5 (HYRAS) and 24.5 d (RADKLIM).

tations (CDO; Python code only based on *xarray* and *numpy* (Harris et al., 2020; Hoyer and Hamman, 2017).

We therefore rule out computational artefacts and proceed to investigate the physical origin of the brushstroke-like structures. Figure 2 shows zoomed-in excerpts of two locations in Fig. 1b where neighbouring grid cells exhibit abrupt CDD transitions. Inspection of the underlying daily precipitation time series reveals that adjacent cells are generally in close agreement, but isolated precipitation events marginally exceeding the 1 mm d^{-1} threshold at one cell – but not its immediate neighbour – are sufficient to interrupt the CDD sequence and produce the sharp spatial discontinuities. This sensitivity to the threshold is an inherent characteristic of the CDD metric rather than a model artefact; applying alternative thresholds (0.1 mm d^{-1}; 2 mm d^{-1}) yields qualitatively similar spatial patterns (see Fig. S2). The same mechanism produces the brushstrokes in RADKLIM (Fig. S5).

Given that ERA5 lacks the resolution to represent such fine-scale CDD variability, the remainder of the analysis focuses on the three high-resolution datasets. To objectively quantify the spatial heterogeneity suggested by Fig. 1, the analysis is restricted to the common spatial extent of COSMO-CLM, HYRAS, and RADKLIM. The spatial autocorrelogram (Fig. 3a) and the RAPSD (Fig. 3b) confirm the visual impression from Fig. 1b–d: COSMO-CLM and RADKLIM exhibit a similar autocorrelation and variance struc-

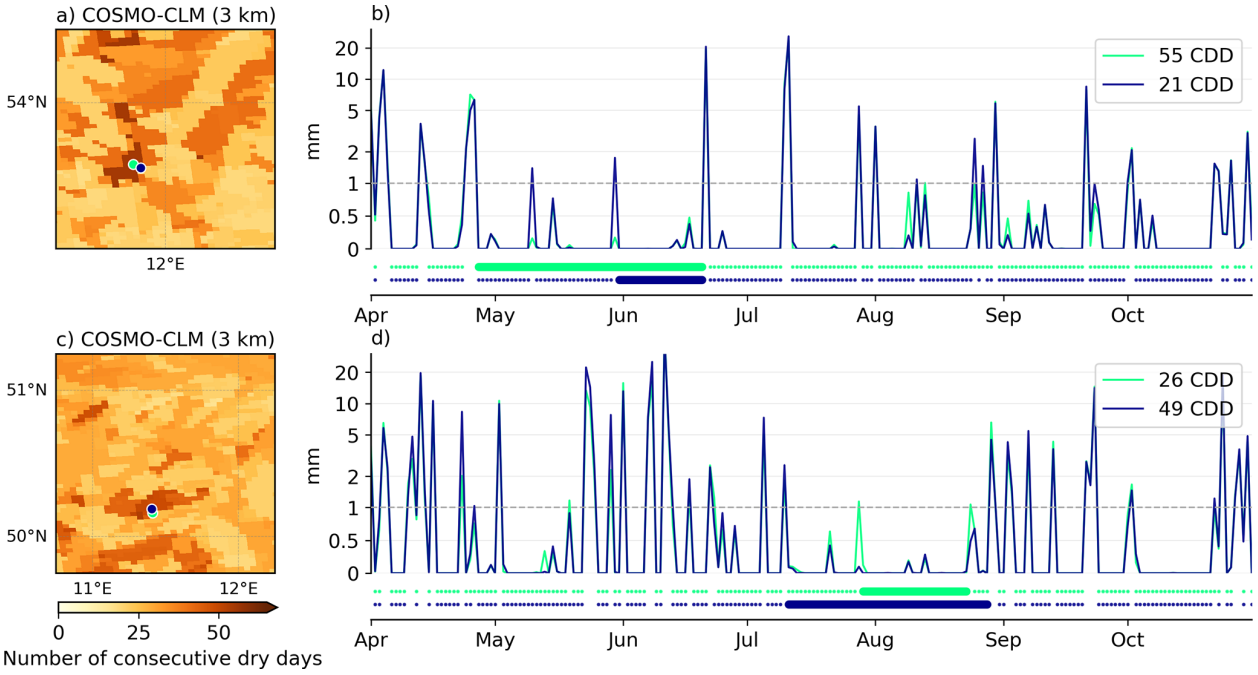


Figure 2. Number of consecutive dry days in 2018 for COSMO-CLM in two regions **(a, c)** and time series of daily precipitation **(b, d)** at the two neighbouring grid cells marked in **(a)** and **(c)**. The dots in **(b)** and **(d)** mark dry days below the threshold of 1 mm, where the thick line highlights the longest spell of consecutive dry days. Note the scaling of the *y*-axis, which is linear below 1 mm and logarithmic above 1 mm.

ture, while HYRAS shows consistently higher spatial autocorrelation across all scales and lower variance especially below wavelengths of 20 km, consistent with the smoother, interpolation-driven pattern seen in Fig. 1c.

4 Lessons for the investigation of consecutive dry days

ERA5 is generally well-suited to reproducing the large-scale characteristics of droughts (Keune et al., 2025), whereas small-scale features such as storm tracks interrupting dry spells are not captured by ERA5 within the CDD metric. Coarse-resolution climate models are known to overestimate the frequency of low-intensity precipitation events – a phenomenon referred to as drizzle bias. Consistent with this, ERA5 has been shown to overestimate precipitation on nominally dry days (Lavers et al., 2022), resulting in an inflated number of wet days (Bandhauer et al., 2022) and a consequent underestimation of CDD. Part of this difference stems from the grid spacing: averaging the COSMO-CLM precipitation to 30 km before computing CDD reduces its mean over Germany from 26.8 to 24.5 d, compared with 21.0 d in ERA5 (Sect. S3). Although HYRAS is derived from about 2100 rain gauges in Germany (one gauge per 172 km^2 in 2018, with a median distance of 8.6 km to the nearest gauge), the bull's-eye anomalies in CDD are attributed here to the interpolation, which preserves daily precipitation at gauge locations but produces bull's-eye patterns around single gauges and spreads small amounts into the surrounding grid cells (Rauthe et al., 2013), a known property of inverse distance weighting (Cressie, 1993).

As a radar-based product, RADKLIM provides spatially consistent coverage, though it is subject to uncertainties and errors inherent to indirect measurement approaches (Kreklow et al., 2020). In a comparison with rain gauges, Kreklow et al. (2020) found that RADKLIM underestimates the frequency of low-intensity precipitation events (hourly intensities below 1 mm h^{-1}), owing to overcorrection of low-reflectivity signals during clutter removal and to shading effects, whereby the radar beam is blocked or attenuated by intervening areas of more intense precipitation. Nevertheless, spatial patterns are generally well reproduced, and the mean CDD of RADKLIM over the common domain differs from that of HYRAS by less than 0.1 d (Fig. 1).

We argue that the brushstroke pattern in CDD arises from precipitation events and convective storm tracks exceeding the 1 mm d^{-1} threshold that are resolved by both radar observations and convection-permitting simulations. We therefore assume that CPMs are capable of reproducing the fine-scale spatial statistics of CDD: the free-running CPM agrees with the independent radar product (Fig. 3; Sect. S5), and rain gauges less than 10 km apart show a CDD variability similar to that of COSMO-CLM and RADKLIM and higher than that of HYRAS (Sect. S6). While this is a positive finding regarding the capabilities of CPMs, the spatial analysis reveals an issue that leads us to advise caution against applying CDD for the purpose of drought evaluation. When CDD

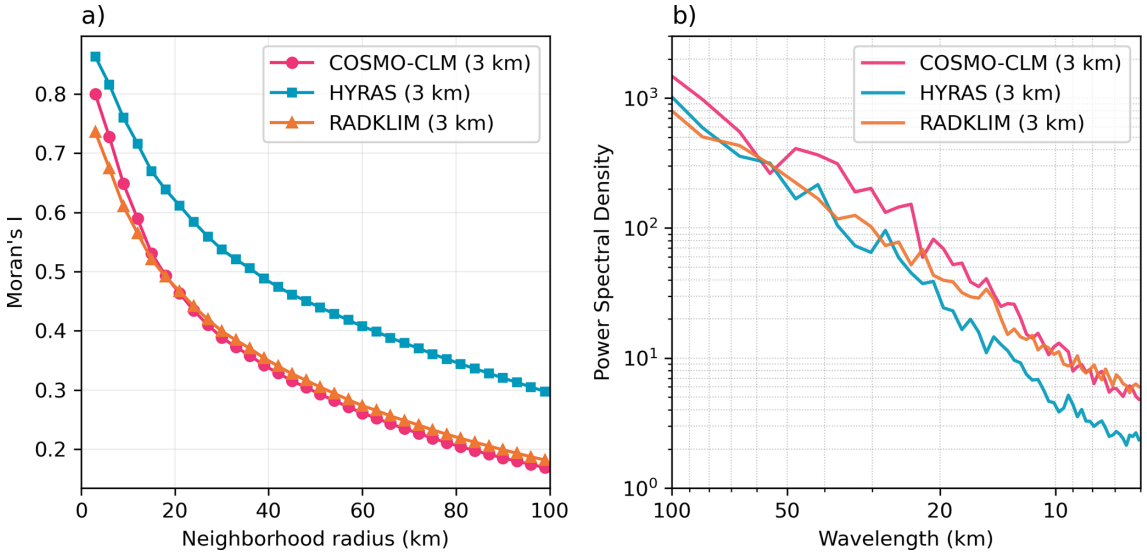


Figure 3. Spatial structure of 2018 CDD fields for COSMO-CLM, HYRAS, and RADKLIM at 3 km resolution. **(a)** Global Moran's I as a function of neighbourhood radius (3–99 km), where higher values indicate stronger spatial autocorrelation. **(b)** Radially averaged power spectral density on the largest square of common valid grid cells (333 km × 333 km) as a function of wavelength, where higher values indicate greater spatial variance at a given scale.

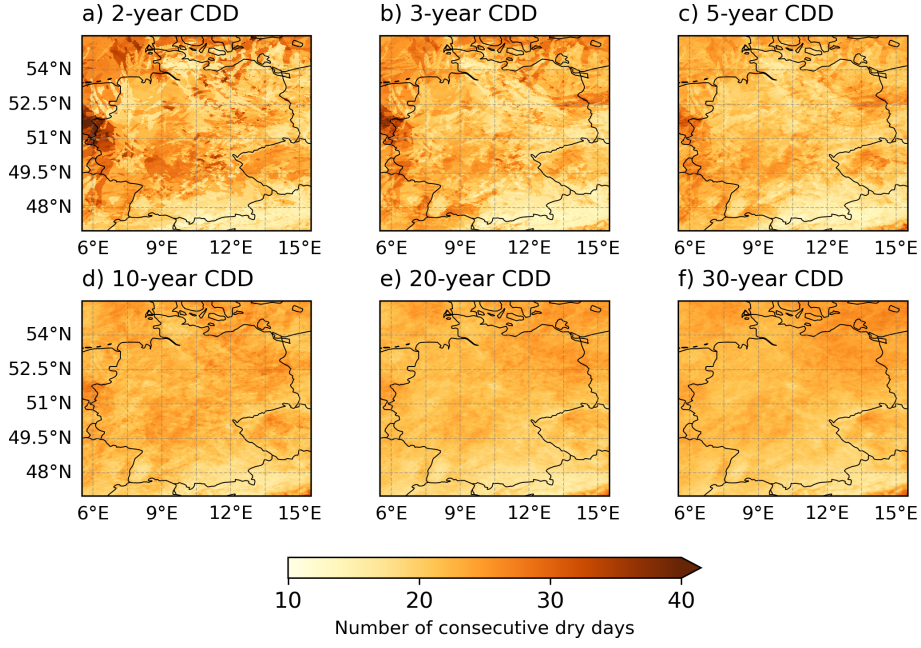


Figure 4. CDD from the COSMO-CLM simulation based on 2 **(a)**, 3 **(b)**, 5 **(c)**, 10 **(d)**, 20 **(e)**, and 30 **(f)** years. Years are selected as 2017–2018, 2016–2018, 2014– 2018, 2009–2018, 1999–2018, and 1989–2018, respectively. Note that the colour scaling is narrower than in Figs. 1 and 2.

are averaged over multiple years (Fig. 4), the chaotic brush-stroke patterns diminish, and the dominant spatial structure reflects large-scale climatic gradients as well as finer-scale topographic influences (Fig. 4f). Nevertheless, multi-year CDD metrics are built upon annual CDD values, which – as demonstrated here – can differ substantially across datasets and are dominated by whether a threshold-exceeding precipitation event happened to occur at a given location in a given year. This sensitivity stems from the run-length definition combined with the threshold as the numbers of dry days are much smoother (Sect. S4). This behaviour is not merely a problem of short averaging windows: a metric whose indi-

vidual realisations are governed by the stochastic occurrence of near-threshold events provides a fundamentally unstable foundation for climatological analysis, regardless of the temporal aggregation applied. For instance, the two neighbouring cells in Fig. 2b differ by 34 d in CDD, although they received 143 and 149 mm from April to October. In COSMO-CLM and RADKLIM, 70 % and 84 % of the adjacent cells whose CDD differ by at least 10 d are separated by events below 2 mm (Sect. S7). Furthermore, this noise does not vanish when CDD is directly derived from point-scale rain gauge records – which is what the ETCCDI were originally designed for: a gauge records the local CDD, but with one gauge per 172 km^2, a station network samples rather than maps the fine-scale variability documented here, and the apparent (dis-)agreement between station records and gridded CDD may be coincidental rather than physically meaningful.

Hence, as our lesson learnt, CDD is not a resolution-independent property of the local climate: coarse grids yield the shorter dry spells of area-mean precipitation, whereas kilometre-scale CDD at a single location is often decided by one event close to the threshold. CDD should therefore only be compared between data sets of similar resolution and be interpreted with caution at individual locations in dry spell monitoring, drought impact and low-flow analyses, and climate model evaluation (e.g. with CDD as part of the ESMValTool; Weigel et al., 2021), whereas its spatial variability may serve as a diagnostic of precipitation intermittency.

Code and data availability. The data and code for this study are openly available on Zenodo (https://doi.org/10.5281/ZENODO.21219565, Poschlod, 2026). ERA5 reanalysis data is available from Copernicus CDS (https://doi.org/10.24381/cds.4991cf48, Copernicus Climate Change Service, 2024). HYRAS and RADKLIM are available from the German Weather Service via https://opendata.dwd.de/climate_environment/CDC/grids_germany/daily/hyras_de/precipitation/ (last access: 19 October 2026) and https://opendata.dwd.de/climate_environment/CDC/grids_germany/hourly/radolan/reproc/2017_002/netCDF/ (last access: 19 October 2026). The COSMO-CLM simulations are openly available at https://doi.org/10.5676/DWD/HOKLISIM_V2022.01 (Brienen et al., 2022). Daily rain gauge data are available from the German Weather Service via https://opendata.dwd.de/climate_environment/CDC/observations_germany/climate/daily/more_precip/historical/ (last access: 19 October 2026).

Supplement. The supplement related to this article is available online at https://doi.org/10.5194/hess-30-7257-2026-supplement.

Author contributions. BP and JS had the idea to assess CDD in convection-permitting simulations. BP conceptualized the study. BP prepared data and software. BP created the figures and prepared the manuscript with contributions from all co-authors.

Competing interests. The contact author has declared that none of the authors has any competing interests.

Disclaimer. Publisher's note: Copernicus Publications remains neutral with regard to jurisdictional claims made in the text, published maps, institutional affiliations, or any other geographical representation in this paper. The authors bear the ultimate responsibility for providing appropriate place names. Views expressed in the text are those of the authors and do not necessarily reflect the views of the publisher.

Acknowledgements. We cordially acknowledge open access to the four data sets used in the study. The authors thank Ingrid Matanić for her contributions to the early analysis carried out during her Master's thesis work supervised by BP and JS. We are grateful to the reviewers Jonathan Wille, Eleonora Dallan, Marc Lemus-Canovas for their helpful comments and feedback as well as to the community comment by Sivarajah Mylevaganam. The authors used Claude Opus 4.8 and Opus 5.5 by Anthropic to assist with the code development and to improve the readability of the text.

Financial support. This research has been supported by the Deutsche Forschungsgemeinschaft (grant no. 390683824).

Review statement. This paper was edited by Manuela Irene Brunner and reviewed by Jonathan Wille, Eleonora Dallan, and Marc Lemus-Canovas.

References

AghaKouchak, A., Huning, L. S., Sadegh, M., Qin, Y., Markonis, Y., Vahedifard, F., Love, C. A., Mishra, A., Mehran, A., Obringer, R., Hjelmstad, A., Pallickara, S., Jiwa, S., Hanel, M., Zhao, Y., Pendergrass, A. G., Arabi, M., Davis, S. J., Ward, P. J., Svoboda, M., Pulwarty, R., and Kreibich, H.: Toward impact-based monitoring of drought and its cascading hazards, Nat. Rev. Earth Environ., 4, 582–595, https://doi.org/10.1038/s43017-023-00457-2, 2023.

Akinsanola, A. A., Jung, C., Wang, J., and Kotamarthi, V. R.: Evaluation of precipitation across the contiguous United States, Alaska, and Puerto Rico in multi-decadal convection-permitting simulations, Sci. Rep., 14, 1238, https://doi.org/10.1038/s41598-024-51714-3, 2024.

Ban, N., Caillaud, C., Coppola, E., Pichelli, E., Sobolowski, S., Adinolfi, M., Ahrens, B., Alias, A., Anders, I., Bastin, S., Belušić, D., Berthou, S., Brisson, E., Cardoso, R. M., Chan, S. C., Christensen, O. B., Fernández, J., Fita, L., Frisius, T., Gašparac, G., Giorgi, F., Goergen, K., Haugen, J. E., Hodnebrog, Ø., Kartsios, S., Katragkou, E., Kendon, E. J., Keuler, K., Lavin-Gullon, A., Lenderink, G., Leutwyler, D., Lorenz, T., Maraun, D., Mercogliano, P., Milovac, J., Panitz, H.-J., Raffa, M., Remedio, A. R., Schär, C., Soares, P. M. M., Srnec, L., Steensen, B. M., Stocchi, P., Tölle, M. H., Truhetz, H., Vergara-Temprado, J., De

Vries, H., Warrach-Sagi, K., Wulfmeyer, V., and Zander, M. J.: The first multi-model ensemble of regional climate simulations at kilometer-scale resolution, part I: evaluation of precipitation, Clim. Dyn., 57, 275–302, https://doi.org/10.1007/s00382-021-05708-w, 2021.

Bandhauer, M., Isotta, F., Lakatos, M., Lussana, C., Båserud, L., Izsák, B., Szentes, O., Tveito, O. E., and Frei, C.: Evaluation of daily precipitation analyses in E-OBS (v19.0e) and ERA5 by comparison to regional high-resolution datasets in European regions, Int. J. Climatol., 42, 727–747, https://doi.org/10.1002/joc.7269, 2022.

Blauhut, V., Stoelzle, M., Ahopelto, L., Brunner, M. I., Teutschbein, C., Wendt, D. E., Akstinas, V., Bakke, S. J., Barker, L. J., Bartošová, L., Briede, A., Cammalleri, C., Kalin, K. C., De Stefano, L., Fendeková, M., Finger, D. C., Huysmans, M., Ivanov, M., Jaagus, J., Jakubínský, J., Krakovska, S., Laaha, G., Lakatos, M., Manevski, K., Neumann Andersen, M., Nikolova, N., Osuch, M., van Oel, P., Radeva, K., Romanowicz, R. J., Toth, E., Trnka, M., Urošev, M., Urquijo Reguera, J., Sauquet, E., Stevkov, A., Tallaksen, L. M., Trofimova, I., Van Loon, A. F., van Vliet, M. T. H., Vidal, J.-P., Wanders, N., Werner, M., Willems, P., and Živković, N.: Lessons from the 2018–2019 European droughts: a collective need for unifying drought risk management, Nat. Hazards Earth Syst. Sci., 22, 2201–2217, https://doi.org/10.5194/nhess-22-2201-2022, 2022.

Bourgault, P., Huard, D., Smith, T. J., Logan, T., Aoun, A., Lavoie, J., Dupuis, É., Rondeau-Genesse, G., Alegre, R., Barnes, C., Laperrière, A. B., Biner, S., Caron, D., Ehbrecht, C., Fyke, J., Keel, T., Labonté, M.-P., Lierhammer, L., Low, J.-F., Quinn, J., Roy, P., Squire, D., Stephens, A., Tanguy, M., and Whelan, C.: xclim: xarray-based climate data analytics, JOSS, 8, 5415, https://doi.org/10.21105/joss.05415, 2023.

Brienen, S., Haller, M., Brauch, J., Früh, B., and Deutscher Wetterdienst: HoKliSim-De (1.0), DWD [data set], https://doi.org/10.5676/DWD/HOKLISIM_V2022.01, 2022.

Brunner, L., Poschlod, B., Dutra, E., Fischer, E. M., Martius, O., and Sillmann, J.: A global perspective on the spatial representation of climate extremes from km-scale models, Environ. Res. Lett., 20, 074054, https://doi.org/10.1088/1748-9326/ade1ef, 2025.

Collier, E. and Mölg, T.: BAYWRF: a high-resolution present-day climatological atmospheric dataset for Bavaria, Earth Syst. Sci. Data, 12, 3097–3112, https://doi.org/10.5194/essd-12-3097-2020, 2020.

Copernicus Climate Change Service: ERA5 post-processed daily-statistics on single levels from 1940 to present, Copernicus Climate Change Service (C3S) Climate Data Store (CDS) [data set], https://doi.org/10.24381/cds.4991cf48, 2024.

Cressie, N. A. C.: Statistics for spatial data, Wiley, New York, 900 pp., https://doi.org/10.1002/9781119115151, 1993.

Dallan, E., Marra, F., Fosser, G., Marani, M., Formetta, G., Schär, C., and Borga, M.: How well does a convection-permitting regional climate model represent the reverse orographic effect of extreme hourly precipitation?, Hydrol. Earth Syst. Sci., 27, 1133–1149, https://doi.org/10.5194/hess-27-1133-2023, 2023.

Gebrechorkos, S. H., Peng, J., Dyer, E., Miralles, D. G., Vicente-Serrano, S. M., Funk, C., Beck, H. E., Asfaw, D. T., Singer, M. B., and Dadson, S. J.: Global high-resolution drought indices for 1981–2022, Earth Syst. Sci. Data, 15, 5449–5466, https://doi.org/10.5194/essd-15-5449-2023, 2023.

Gutowski, W. J., Ullrich, P. A., Hall, A., Leung, L. R., O'Brien, T. A., Patricola-DiRosario, C. M., Arritt, R. W., Bukovsky, M. S., Calvin, K. V., Feng, Z., Jones, A. D., Kooperman, G. J., Monier, E., Pritchard, M. S., Pryor, S. C., Qian, Y., Rhoades, A. M., Roberts, A. F., Sakaguchi, K., Urban, N., and Zarzycki, C.: The Ongoing Need for High-Resolution Regional Climate Models: Process Understanding and Stakeholder Information, Bull. Am. Meteorol. Soc., 101, E664–E683, https://doi.org/10.1175/BAMS-D-19-0113.1, 2020.

Harris, C. R., Millman, K. J., Van Der Walt, S. J., Gommers, R., Virtanen, P., Cournapeau, D., Wieser, E., Taylor, J., Berg, S., Smith, N. J., Kern, R., Picus, M., Hoyer, S., Van Kerkwijk, M. H., Brett, M., Haldane, A., Del Río, J. F., Wiebe, M., Peterson, P., Gérard-Marchant, P., Sheppard, K., Reddy, T., Weckesser, W., Abbasi, H., Gohlke, C., and Oliphant, T. E.: Array programming with NumPy, Nature, 585, 357–362, https://doi.org/10.1038/s41586-020-2649-2, 2020.

Hentgen, L., Ban, N., Kröner, N., Leutwyler, D., and Schär, C.: Clouds in Convection-Resolving Climate Simulations Over Europe, JGR Atmos., 124, 3849–3870, https://doi.org/10.1029/2018JD030150, 2019.

Hersbach, H., Bell, B., Berrisford, P., Hirahara, S., Horányi, A., Muñoz-Sabater, J., Nicolas, J., Peubey, C., Radu, R., Schepers, D., Simmons, A., Soci, C., Abdalla, S., Abellan, X., Balsamo, G., Bechtold, P., Biavati, G., Bidlot, J., Bonavita, M., De Chiara, G., Dahlgren, P., Dee, D., Diamantakis, M., Dragani, R., Flemming, J., Forbes, R., Fuentes, M., Geer, A., Haimberger, L., Healy, S., Hogan, R. J., Hólm, E., Janisková, M., Keeley, S., Laloyaux, P., Lopez, P., Lupu, C., Radnoti, G., De Rosnay, P., Rozum, I., Vamborg, F., Villaume, S., and Thépaut, J.: The ERA5 global reanalysis, Quart. J. Royal Meteorol. Soc., 146, 1999–2049, https://doi.org/10.1002/qj.3803, 2020.

Hoyer, S. and Hamman, J.: xarray: N-D labeled Arrays and Datasets in Python, JORS, 5, 10, https://doi.org/10.5334/jors.148, 2017.

Intergovernmental Panel On Climate Change (IPCC): Climate Change 2021 – The Physical Science Basis: Working Group I Contribution to the Sixth Assessment Report of the Intergovernmental Panel on Climate Change, 1st ed., Cambridge University Press, https://doi.org/10.1017/9781009157896, 2023.

Karki, R., ul Hasson, S., Gerlitz, L., Schickhoff, U., Scholten, T., and Böhner, J.: Quantifying the added value of convection-permitting climate simulations in complex terrain: a systematic evaluation of WRF over the Himalayas, Earth Syst. Dynam., 8, 507–528, https://doi.org/10.5194/esd-8-507-2017, 2017.

Kchouk, S., Melsen, L. A., Walker, D. W., and van Oel, P. R.: A geography of drought indices: mismatch between indicators of drought and its impacts on water and food securities, Nat. Hazards Earth Syst. Sci., 22, 323–344, https://doi.org/10.5194/nhess-22-323-2022, 2022.

Kendon, E. J., Prein, A. F., Senior, C. A., and Stirling, A.: Challenges and outlook for convection-permitting climate modelling, Phil. Trans. R. Soc. A., 379, 20190547, https://doi.org/10.1098/rsta.2019.0547, 2021.

Keune, J., Di Giuseppe, F., Barnard, C., Damasio Da Costa, E., and Wetterhall, F.: ERA5–Drought: Global drought indices based on ECMWF reanalysis, Sci. Data, 12, 616, https://doi.org/10.1038/s41597-025-04896-y, 2025.

Kreklow, J., Tetzlaff, B., Burkhard, B., and Kuhnt, G.: Radar-Based Precipitation Climatology in Germany—Developments,

Uncertainties and Potentials, Atmosphere, 11, 217, https://doi.org/10.3390/atmos11020217, 2020.

Lavers, D. A., Simmons, A., Vamborg, F., and Rodwell, M. J.: An evaluation of ERA5 precipitation for climate monitoring, Quart. J. Royal Meteorol. Soc., 148, 3152–3165, https://doi.org/10.1002/qj.4351, 2022.

Lind, P., Belušić, D., Christensen, O. B., Dobler, A., Kjellström, E., Landgren, O., Lindstedt, D., Matte, D., Pedersen, R. A., Toivonen, E., and Wang, F.: Benefits and added value of convection-permitting climate modeling over Fenno-Scandinavia, Clim. Dyn., 55, 1893–1912, https://doi.org/10.1007/s00382-020-05359-3, 2020.

Liu, Y., Shan, F., Yue, H., Wang, X., and Fan, Y.: Global analysis of the correlation and propagation among meteorological, agricultural, surface water, and groundwater droughts, J. Environ. Manage., 333, 117460, https://doi.org/10.1016/j.jenvman.2023.117460, 2023.

Lucas-Picher, P., Argüeso, D., Brisson, E., Tramblay, Y., Berg, P., Lemonsu, A., Kotlarski, S., and Caillaud, C.: Convection-permitting modeling with regional climate models: Latest developments and next steps, WIREs Clim. Change, 12, e731, https://doi.org/10.1002/wcc.731, 2021.

Molina, M. O., Careto, J. M., Gutiérrez, C., Sánchez, E., Goergen, K., Sobolowski, S., Coppola, E., Pichelli, E., Ban, N., Belušić, D., Short, C., Caillaud, C., Dobler, A., Hodnebrog, Ø., Kartsios, S., Lenderink, G., De Vries, H., Göktürk, O., Milovac, J., Feldmann, H., Truhetz, H., Demory, M. E., Warrach-Sagi, K., Keuler, K., Adinolfi, M., Raffa, M., Tölle, M., Sieck, K., Bastin, S., and Soares, P. M. M.: The added value of simulated near-surface wind speed over the Alps from a km-scale multimodel ensemble, Clim. Dyn., 62, 4697–4715, https://doi.org/10.1007/s00382-024-07257-4, 2024.

Monteiro, D., Caillaud, C., Lafaysse, M., Napoly, A., Fructus, M., Alias, A., and Morin, S.: Improvements in the land surface configuration to better simulate seasonal snow cover in the European Alps with the CNRM-AROME (cycle 46) convection-permitting regional climate model, Geosci. Model Dev., 17, 7645–7677, https://doi.org/10.5194/gmd-17-7645-2024, 2024.

Petrova, I. Y., Miralles, D. G., Brient, F., Donat, M. G., Min, S.-K., Kim, Y.-H., and Bador, M.: Observation-constrained projections reveal longer-than-expected dry spells, Nature, 633, 594–600, https://doi.org/10.1038/s41586-024-07887-y, 2024.

Poschlod, B.: Data and Code for: LESSONS report: Fine-scale representation of consecutive dry days, Zenodo [data set and code], https://doi.org/10.5281/ZENODO.21219565, 2026.

Poschlod, B. and Daloz, A. S.: Snow depth in high-resolution regional climate model simulations over southern Germany – suitable for extremes and impact-related research?, The Cryosphere, 18, 1959–1981, https://doi.org/10.5194/tc-18-1959-2024, 2024.

Poschlod, B. and Koh, J.: Convection-Permitting Climate Models Can Support Observations to Generate Rainfall Return Levels, Water Res. Resour., 60, e2023WR035159, https://doi.org/10.1029/2023WR035159, 2024.

Pulkkinen, S., Nerini, D., Pérez Hortal, A. A., Velasco-Forero, C., Seed, A., Germann, U., and Foresti, L.: Pysteps: an open-source Python library for probabilistic precipitation nowcasting (v1.0), Geosci. Model Dev., 12, 4185–4219, https://doi.org/10.5194/gmd-12-4185-2019, 2019.

Rauthe, M., Steiner, H., Riediger, U., Mazurkiewicz, A., and Gratzki, A.: A Central European precipitation climatology Part I: Generation and validation of a high-resolution gridded daily data set (HYRAS), METZ, 22, 235–256, https://doi.org/10.1127/0941-2948/2013/0436, 2013.

Ravuri, S., Lenc, K., Willson, M., Kangin, D., Lam, R., Mirowski, P., Fitzsimons, M., Athanassiadou, M., Kashem, S., Madge, S., Prudden, R., Mandhane, A., Clark, A., Brock, A., Simonyan, K., Hadsell, R., Robinson, N., Clancy, E., Arribas, A., and Mohamed, S.: Skilful precipitation nowcasting using deep generative models of radar, Nature, 597, 672–677, https://doi.org/10.1038/s41586-021-03854-z, 2021.

Rybka, H., Haller, M., Brienen, S., Brauch, J., Früh, B., Junghänel, T., Lengfeld, K., Walter, A., and Winterrath, T.: Convection-permitting climate simulations with COSMO-CLM for Germany: Analysis of present and future daily and sub-daily extreme precipitation, METZ, 32, 91–111, https://doi.org/10.1127/metz/2022/1147, 2023.

Schulzweida, U.: CDO Release 2.6.0, https://code.mpimet.mpg.de/projects/cdo/embedded/cdo.pdf (last access: 19 October 2026), 2026.

Sinclair, S. and Pegram, G. G. S.: Empirical Mode Decomposition in 2-D space and time: a tool for space-time rainfall analysis and nowcasting, Hydrol. Earth Syst. Sci., 9, 127–137, https://doi.org/10.5194/hess-9-127-2005, 2005.

Van Loon, A. F. and Van Lanen, H. A. J.: A process-based typology of hydrological drought, Hydrol. Earth Syst. Sci., 16, 1915–1946, https://doi.org/10.5194/hess-16-1915-2012, 2012.

Weigel, K., Bock, L., Gier, B. K., Lauer, A., Righi, M., Schlund, M., Adeniyi, K., Andela, B., Arnone, E., Berg, P., Caron, L.-P., Cionni, I., Corti, S., Drost, N., Hunter, A., Lledó, L., Mohr, C. W., Paçal, A., Pérez-Zanón, N., Predoi, V., Sandstad, M., Sillmann, J., Sterl, A., Vegas-Regidor, J., von Hardenberg, J., and Eyring, V.: Earth System Model Evaluation Tool (ESMValTool) v2.0 – diagnostics for extreme events, regional and impact evaluation, and analysis of Earth system models in CMIP, Geosci. Model Dev., 14, 3159–3184, https://doi.org/10.5194/gmd-14-3159-2021, 2021.

Wille, J. D., Koch, R., Becker, T., and Fischer, E.: Extreme Precipitation Depiction in Convection-Permitting Earth System Models Within the nextGEMS Project, J. Adv. Model. Earth Syst., 17, e2024MS004840, https://doi.org/10.1029/2024MS004840, 2025.

Winterrath, T., Brendel, C., Hafer, M., Junghänel, T., Klameth, A., Walawender, E., Weigl, E., and Becker, A.: Erstellung einer radargestützten Niederschlagsklimatologie, Berichte des Deutschen Wetterdienstes, 251, DWD, Offenbach am Main, https://opendata.dwd.de/climate_environment/GPCC/radarklimatologie/Dokumente/Endbericht_Radarklimatologie_final.pdf (last access: 6 May 2026), 2017.

Zhang, X., Alexander, L., Hegerl, G. C., Jones, P., Tank, A. K., Peterson, T. C., Trewin, B., and Zwiers, F. W.: Indices for monitoring changes in extremes based on daily temperature and precipitation data, WIREs Clim. Change, 2, 851–870, https://doi.org/10.1002/wcc.147, 2011.